3 Continental collision zones

The following chapter provides a summary of concepts and models thought to describe bivergent wedges. Thereby, special emphasis is devoted to the ability of these models to predict the spatio-temporal distribution of deformation and surface uplift.

3.1 Kinematic concepts of bivergent orogens

Lithosphere-scaled profiles across natural bivergent orogens such as the European Alps, the Pyrenees or Taiwan (Fig. 3.1) have several phenomena in common, which result from the asymmetry associated with the convergence geometry, i. e., the presence of a downgoing and an overriding plate. This asymmetry forms the basis for the key kinematic assumption that collisional orogens result from the partial subduction of continental lithosphere and accretion of crustal material (Willett et al., 1993; Ellis et al., 1995; Ellis, 1996). According to Willett et al. (1993) a velocity discontinuity (singularity) separates the subducting (lower) plate from the overriding (upper) plate and forms thus the lower limit of accretion (Fig. 1.2). The asymmetry of the subduction process evokes a polarity in the resulting crustal mass transfer, i. e., all crustal mass moving into an orogen is derived from the subducting plate and moves towards the overriding plate. This in turn leads to the formation of two crustal sub-wedges. The pro-wedge located upstream of the singularity grows by frontal and basal accretion of lower plate material. In contrast, the retro-wedge located downstream of the singularity develops by translation of pro-wedge material towards the upper plate. The axial-zone is defined as the topographic culmination of the bivergent wedge and changes its position with respect to the singularity through time. Furthermore, both the pro- and the retro-wedge differ also with respect to their topographic gradients. Thereby, the former has a lower and the latter a higher topographic gradient (Willett et al., 1993; Beaumont et al., 1996).

The asymmetry of the convergence geometry evokes also a distinct temporal distribution of deformation. During early stages of collision, deformation is dominantly located within the pro-wedge, but migrates towards the upper plate during a late collisional-stage (Willett et al., 1993; Beaumont et al., 1996). A further key observation, which emerges from the above cross-sections, is the flexural downbending of the involved lithospheres during continental collision. Thus, a successful simulation of bivergent wedges should provide the key characteristics indicated above.

3.2 Kinematic models of fold and thrust belts

One of the critical issues in the analysis of fold and thrust belts, is the timing of thrusting and several models have been put forward to explain the variability found in nature (Storti et al., 2000; Butler, 2004). These are:

i. Forward breaking piggy-back thrusting (Boyer and Elliott, 1982), where displacement is transferred onto a new thrust initiated in the footwall of the previously active thrust (Fig. 3.2a). The latter is abandoned and passively carried in the hangingwall of the former (Butler, 1987). Thus, deformation propagates systematically from the hinterland towards the foreland.

ii. Break-back thrusting (Butler, 1987), where a sole thrust propagates into the foreland, followed by the formation of major thrusts
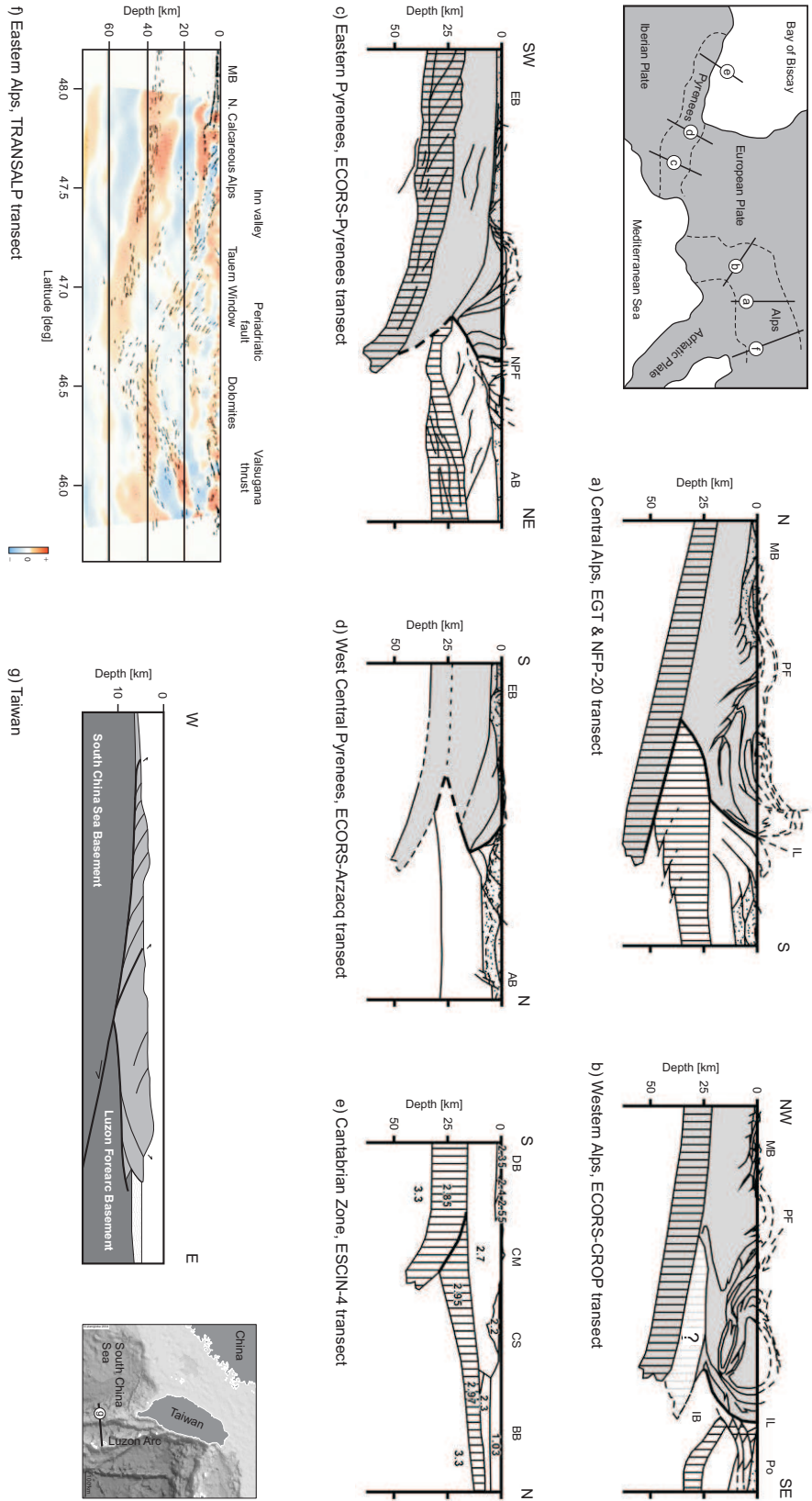
Figure 3.1: Crustal scaled cross-sections of bivergent orogens: (a) Central Alps; (b) Western Alps. The area with gray vertical ruling represents imbricated European lower crust; (c) Eastern Pyrenees; (d) West Central Pyrenees; (e) Cantabrian Zone, densities are listed in g/cm^3; (f) Eastern Alps; (g) Taiwan. Cross sections (a) - (e) are based on deep seismic reflection, refraction and gravity . Cross section (f) is based on seismic reflection and receiver functions, cross section (g) on seismic reflection. No vertical exaggeration. Gray represents the downgoing and white the overriding plate. Vertical ruling in (a) - (e) indicates a reflective and high velocity or density (e.g., $> 6.5 km/s$; $2900 kg/m$) layer commonly associated with the mafic lower crust. Dot pattern represents foreland sedimentary deposits. Dashed lines indicate eroded features or lack of control. AB, Aquitaine basin; BB, Bay of Biscay; CM, Cantabrian mountains; CS, Cantabrian shelf; DB, Duero basin; EB, Ebro basin; IB, Ivrea Body; IL, Insubric Line; MB, Molasse basin; PF, Penninic front; Po, Po basin. (a) - (e) modified after Moore and Wiltschko (2004), (f) after Kummerow et al. (2004) and (g) after Malavielle et al. (2002). Taiwan map created with www.planiglobe.com.

above it (Fig. 3.2b). Thereby, successively younger thrusts are formed towards the hinterland (Morley, 1988).

iii. In-sequence thrusting, where a thrust sequence has formed progressively in one direction, which can either be a forward- or a break-back sequence (McClay, 1992).

iv. Out-of-sequence thrusting (Morley, 1988; McClay, 1992), where the sequence of thrusting does not conform with either a progressive forward- or break-back sequence. Morley (1988) distinguished three modes of out-of-sequence thrusting: the re-activation of an older thrust (Fig. 3.2c), synchronous thrusting (Boyer, 1992; Storti et al., 2000), where two or more thrust accumulate displacement at the same time (Fig. 3.2d) and the formation of a new thrust which cuts through and displaces pre-existing thrusts (Fig. 3.2e).

Whether forward breaking, break-back, in sequence or out-of-sequence thrusting occurs is commonly attributed to local factors such as mechanic stratigraphy, syntectonic erosion, sedimentation or basement fabrics (Storti et al., 2000). Storti et al. (2000) showed also that several of the above "thrust-modes" can act at the same time. This is thought to result from the complex mechanical balance, which varies through time.

Although, not clearly stated, the above conceptual models involve some predictions of how displacement is partitioned in space and time. Henry Cadell (1888) was probably the first to note that the slip along the deformation front depends on the phase within the accretion cycle, a term not known in his days. Cadell (1888) showed that *at one point, the brittle strata snapped, i. e., a thrust was formed, and all the movement was concentrated along the line of weakness thus produced. The whole mass above this thrust-plane moved obliquely upwards and forwards, and all interstitial movement ceased.* Similarly, Mulugeta and
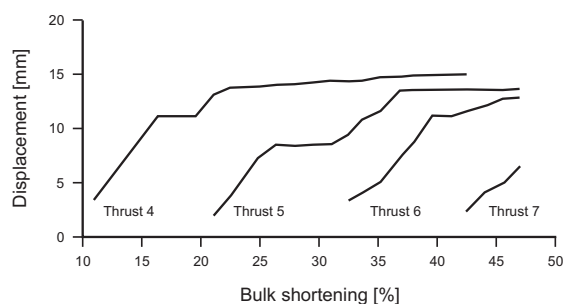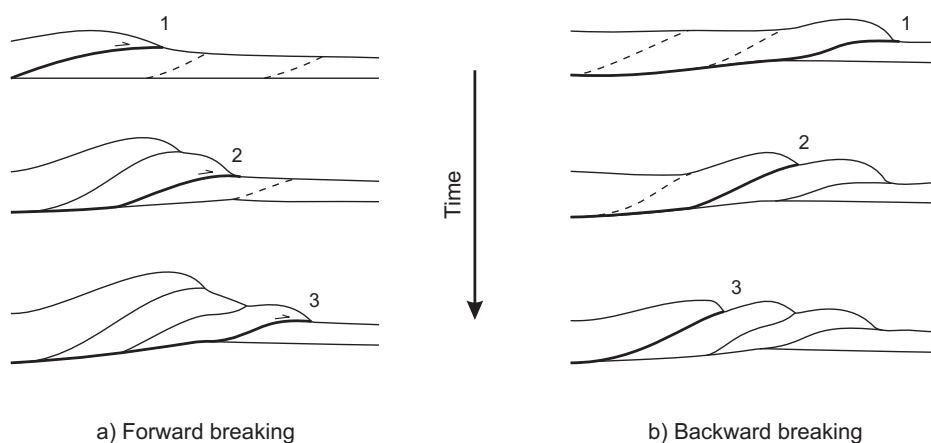

Figure 3.3: Displacement versus bulk shortening of four thrusts taken from Koyi (1995). Evolution of displacement of all imbricates follows a similar pattern; starting with a sharp increase as the imbricate begins to form, followed by little or no additional displacement before the formation of a new imbricate in front of the former. This in turn is followed by a gentler increase in displacement that decreases significantly with progressive deformation.

Koyi (1992) found that lateral growth of an accretionary wedge is episodic and Koyi (1995) suggested that each accretion episode is predated by a stepwise increase of the height of the wedge. Furthermore, Koyi (1995) demonstrated that displacement rate along thrusts is not constant through time and that three phases can be distinguished. During the first phase, i. e., the initiation of an imbricate, displacement rate is high, followed by a period of quiescence, during which a new thrust is formed in the foreland. In the third phase a slight increase of the displacement rate, which is lower than the one in the first phase can be observed. Finally, displacement rate approaches zero with continued convergence (Fig. 3.3). This result suggests thus that displacement is partitioned in space and time. Experimental observations and minimum work calculations by Gutscher et al. (1998) provided additional support for the cyclic nature of accretion. Similar to Koyi (1995) they found that (i) the maximum uplift migrates systematically backwards during an accretion cycle and that (ii) the main backthrust accommodates most of its slip at the end of each accretion cycle, which lead Gutscher et al. (1998) to conclude that each accretion cycle consists of two phases: the thrust initiation and the underthrust-

End-member modes of thrust sequences

a) Forward breaking   b) Backward breaking

Modes of out-of-sequence thrusting

c) Re-activation of a thrust   d) Synchronous thrusting   e) Creation of a new thrust
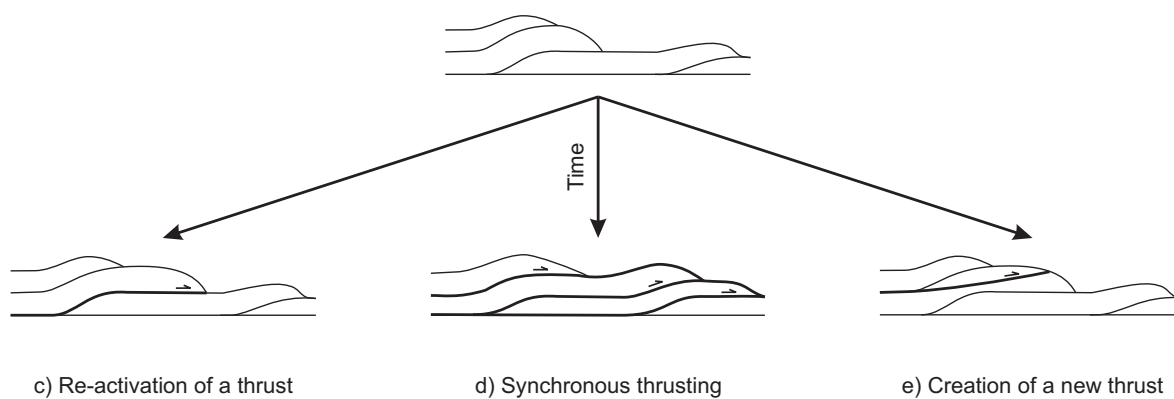
Figure 3.2: End-member modes of thrust sequences, modified after Morley (1988). (a) Forward or piggy-back breaking sequence, where deformation propagates toward the foreland with time. (b) Break-back sequence, where deformation propagates toward the hinterland with time, numbers indicate sequence of activity. Modes of out-of-sequence thrusting: (c) Re-activation of an older thrust located within the wedge. (d) Synchronous thrusting of two or more thrusts. (e) Creation of a new thrust, which cuts across and displaces older ones.
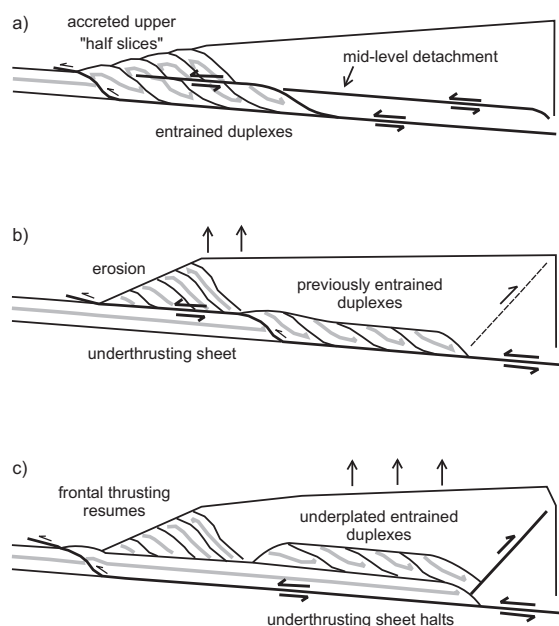
Figure 3.4: Bipartite evolution of an accretion cycle, taken from Gutscher et al. (1998). (a) Frontal accretion with shearing of imbricate slices at a mid-level detachment. (b) Underthrusting with frontal uplift. (c) Underplating of entrained duplexes associated with backthrusting and uplift at the rear of the wedge (vertical arrows indicate maximum uplift). Gutscher et al. (1998) used a high basal friction, i.e., $\mu_b = 0.5$, which is similar to the one used in this study $\mu_{bdynamic} = 0.54$.

ing phase respectively (Fig. 3.4). Such a bipartite evolution has also been documented from sandbox experiments, which simulate oblique convergence (Hoffmann-Rothe et al., 2004). Therefore, both terms, i.e., the thrust initiation phase and the underthrusting phase are adopted in this study.

3.3 The Critical Coulomb Wedge concept

The fundamental dynamic assumption is that a subduction-accretion process leads to the formation of an orogenic wedge with a geometry governed by the relative magnitude of the frictional resistance along the base and the compressive strength of the wedge material (Dahlen, 1990).

Although, considerable natural variations exist among crustal wedges, they exhibit several common properties in cross section. Chapple (1978) pointed out that accretionary wedges as well as fold-and-thrust belts show: (i) a basal detachment or décollement, which dips towards the interior of the mountain belt; (ii) large horizontal compression in the material above and little deformation within the material below the detachment and (iii) a characteristic wedge shape of the deformed material, tapering towards the foreland of the mountain belt. These observations in conjunction with sandbox experiments formed the basis for the critical taper theory (Davis et al., 1983), which was later adopted by various physical and numerical simulation studies for accretionary wedges (Byrne et al., 1993; Kukowski et al., 1994; Lallemand et al., 1994; Gutscher et al., 1996, 1998; Lohrmann et al., 2003), for fold-and-thrust belts (Storti and McClay, 1995; Nieuwland et al., 2000; Cobbold et al., 2001), as well as for doubly vergent wedges (Malavieille, 1984; Wang and Davis, 1996; Willett, 1999; Storti et al., 2000, 2001; Persson et al., 2004; Hoth et al., 2006). In principle, provided crustal deformation is driven by convergence and basal shear stresses are significant, the deforming crust attains a 'critical' balance between gravitational stresses, basal shear stresses and the strength of the crust at the scale of the entire crust, thus resulting in the formation of an 'orogenic wedge' (Platt, 1986).

The overall mechanics of critical Coulomb wedges are commonly considered to be analogous to the mechanics of wedges that form in front of a moving bulldozer or snow plow (Davis et al., 1983) and both models are often cited for intuitive understanding. Accordingly, if a snow plow starts to move through a fresh layer of snow two scenarios can be envisaged. Given that the internal strength of the snow is higher than the friction with the road, e.g., if the snow is icy and the road is warm, then the snow will be moved as an undeformed slab in front of the plow. If

however, the internal strength is smaller than the friction with the road, which is usually the case, then the snow deforms internally and its surface will become inclined. According to the Mohr-Coulomb failure criterion, the strength of the snow will increase as the thickness of the snow wedge increases until a critical taper between the surface slope and the basal detachment (i. e., the road) is reached. At this stage, the strength of the snow is exactly as large as the basal traction and the snow wedge can now move along its base without internal deformation. It follows that a critically tapered snow wedge is the thinnest body that can be thrust over its detachment without internal deformation. While sliding over its base, accretion of new material to a critically tapered snow wedge promotes internal deformation to accommodate the respective influx and to restore the critical taper.

From the above analogy it is evident that the parameters, which determine the failure criterion of the wedge material and its base, control the shape of the wedge. Thus, a failure law must be specified both within the wedge and along its base in order to solve for the state of stress within and for the critical taper of the respective wedge (Dahlen and Suppe, 1988). Generally, stress within the lithosphere is thought to be limited by frictional sliding (Byerlee, 1978) at low confining pressures and by thermally activated processes, especially dislocation creep (Brace and Kohlstedt, 1980) at high temperatures. Therefore, brittle behaviour is thought to be satisfactorily described by the Mohr-Coulomb failure criterion and is considered as the stress-limiting factor (Davis et al., 1983; Dahlen and Suppe, 1988). It can be written as:

$$\tau = \mu(\sigma_N - p_f) + C_0 \qquad (3.1)$$

where τ is the shear strength, C_0 the cohesive strength, μ is the coefficient of internal friction, which relates to the angle of internal friction (ϕ) by $\mu = \tan\phi$, σ_N is the normal stress and p_f the fluid pressure. The form $(\sigma_N - p_f)$ describes the effective normal stress (Hubbert and Rubey,

1959). It follows from equation (3.1) that the Mohr-Coulomb failure criterion is strongly (fluid) pressure-dependent but is largely independent of temperature or strain rate (Byerlee, 1978).

The effect of cohesion on the magnitude of the resulting shear strength and finally on the geometry of the wedge depends on the vertical and horizontal position within the wedge under consideration. At depths on the order of a few kilometers, the effect of cohesion, which is in the order of 1 to $150\,MPa$ (Dahlen and Suppe, 1988), is negligible in comparison with the pressure-dependent term in the failure equation (3.1). According to Davis et al. (1983) the main effects of cohesion on wedge geometry will be observed near the toe of the wedge, where cohesion can add significantly to the total strength and produce a critical taper smaller than the corresponding cohesionless taper. Farther from the toe where the wedge is thicker, the pressure-dependent term dominates, and the critical taper will asymptotically approach the cohesionless value (Davis et al., 1983).

Furthermore, Byerlee (1978) demonstrated that μ is largely independent of lithology but depends on the magnitude of normal stresses. For normal stresses below $200\,MPa$, the shear stress required to induce sliding is given by $\tau = 0.85\,\sigma_N$; above $200\,MPa$, $\tau = 0.6\,\sigma_N$ (Byerlee, 1978).

As indicated above, fluid pressures play a crucial role in controlling the mechanics of thrust faulting. Fluids cannot support shear stresses and their respective pressure has the same magnitude in all directions. Therefore, fluid pressure reduces the magnitude of the principal stresses, but the deviatoric stress remains constant. It follows that the Mohr circle is shifted towards the origin – brittle failure sets in at lower shear stresses. The corresponding angle between σ_1 (highest normal stress) and the failure plane is reduced with respect to the case, where no fluid pressure was present.

From the above description of the controlling failure law it is evident that the lower limit of the

Critical Coulomb wedge (CCW) theory is the middle to lower crust, where pressure and temperature become sufficiently high that common rocks begin to display a temperature-dependent plastic behaviour (Davis et al., 1983). Although the CCW concept was originally formulated for a non-cohesive Mohr-Coulomb type rheology (Davis et al., 1983; Dahlen et al., 1984) presented a solution involving cohesion and Platt (1993) extended this theory to involve perfectly plastic materials.

In the following a short derivation of the critical taper equation is provided. A Cartesian coordinate system is employed, where x is parallel to the base of the wedge and z increases upward (Fig. 3.5). The local thickness of the wedge is given by H_w, measured along the z-axis. Neglecting along-strike variations and assuming plane strain, Davis et al. (1983) proposed that the critical taper of a compressive wedge is controlled by the balance of four forces in the x direction:

The gravitational body force which is given by:

$$F_g = -\rho g H_w dx \sin \beta \qquad (3.2)$$

where ρ, assumed constant, is the density of rocks, g is the acceleration due to gravity, H_w is the height of the wedge and β is the dip of the base with respect to the horizontal. F_g is negative, since it resists movement of the material uphill.

The x-component of the pressure of the water overburden, which resists sliding:

$$F_w = -\rho_w g D dx \sin(\alpha + \beta) \qquad (3.3)$$

where ρ_w is the density of water, D is the height of the water column at x and α is the local angle of topographic relief of the wedge.

The basal shear traction τ_b is negative as well, since it resists sliding and is given by:

$$\tau_b = -\mu_b(1 - \lambda_b)\rho g D H_w \qquad (3.4)$$

where μ_b is the basal coefficient of friction and λ_b is the Hubbert and Rubey pore fluid ratio for the basal detachment. While introducing μ_b and λ_b one allows explicitly for the fact that the basal detachment is a zone of weakness either because of a lower intrinsic strength with respect to the internal strength (μ_0), or because of elevated fluid pressures. For a through-going basal detachment to operate the condition

$$(1 - \lambda_b)\mu_b = (1 - \lambda_0)\mu_0 \qquad (3.5)$$

must be satisfied. Thereby, λ_0 is the internal pore fluid ratio (Davis et al., 1983).

Let $\sigma_x(x, z)$ be the normal traction, which acts across any face perpendicular to the x-axis. Integration of this term with respect to dz at position x delivers the work needed to push the face at position x. However, this is counteracted (actio = re-actio) by a force at $x + dx$ which is somewhat smaller, since z is lower and the respective work resulting from integration is smaller as well. Thus, the difference in work between the position x and $x + dx$, which can be considered as the gradient or the first derivation, is the resultant compressive push in positive x direction. In case $dx > 0$ the above gradient belongs to a secant. Therefore, the limit of $dx \to 0$ is needed to calculate the gradient of the tangent at position x, which is thus the resultant compressive force at position x (Fig. 3.6).

$$F_s = \frac{d}{dx} \int_0^H \sigma_x \, dz \qquad (3.6)$$

Balancing the above four forces to find the condition at which the wedge can be pushed over its base without internal deformation, results in:

$$0 = F_g + F_w + \tau_b + F_s. \qquad (3.7)$$

Equation (3.7) implies that a critically tapered wedge is at the verge of shear failure everywhere, which is the key physical assumption made in the CCW concept. In order to solve for the state of stress within and for the critical taper of the respective wedge, the only remaining unknown quantity is σ_x, which can be determined by using
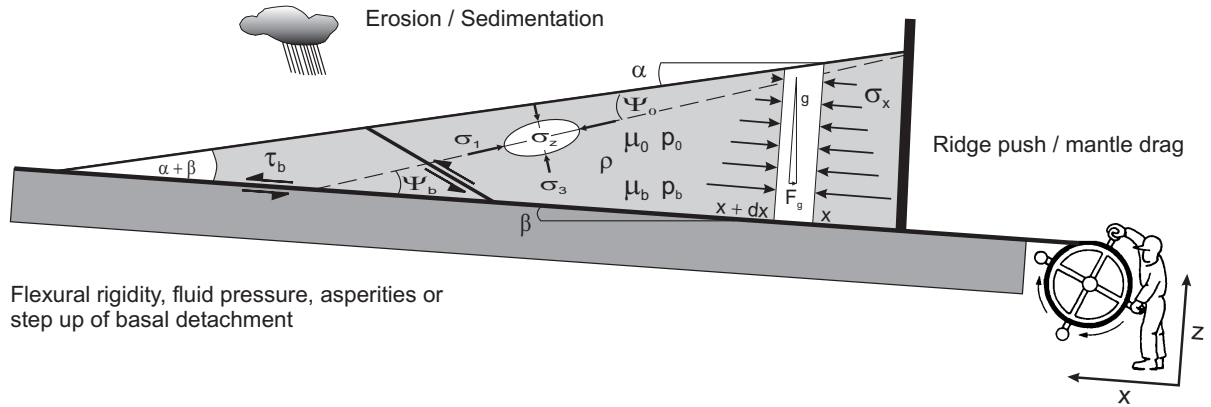
Figure 3.5: Schematic diagram of a subaerial wedge subject to horizontal compression. Terminology used to describe the critical taper equation is provided: α surface slope; β basal dip; μ_0 coefficient of internal friction; μ_b coefficient of basal friction; p_0 internal fluid pressure; p_b basal fluid pressure; ρ density of rocks; σ_1 maximum, σ_3 minimum principal stress; Ψ_0 angle between σ_1 and surface slope; Ψ_b angle between σ_3 and wedge base. The three forces, acting upon an arbitrary wedge-column of width dx are: the gravitational body force and the basal traction resist movement of the material up hill and the push from the rear. For stable sliding of the whole wedge to occur, the force balance has to equate to zero, i. e., a critically tapered wedge is the thinnest body of material, which can slide over its base without internal deformation. Additionally, external processes thought to influence the shape and growth of wedge are indicated. Figure in cap (Dan Davis) not shown to scale. Modified after Davis et al. (1983), Dahlen (1990) and Lohrmann et al. (2003).

a Mohr circle (Davis et al., 1983). After several rearrangements of equation (3.7), small angle approximations as well as the simplifying assumption that $\lambda_0 = \lambda_b$, one finally arrives at the following equation for a submarine wedge:

$$\alpha + \beta = \frac{(1-\lambda_b)\mu_b + (1-\rho_w/\rho)\beta}{(1-\rho_w/\rho) + (1-\lambda)K}. \qquad (3.8)$$

In case of a subaerial wedge ρ_w is set to 0 in equation (3.8). It follows:

$$\alpha + \beta = \frac{(1-\lambda_b)\mu_b + \beta}{1 + (1-\lambda)K}. \qquad (3.9)$$

In case of sandbox experiments where the sand is dry, i. e., $\lambda = 0$ and assuming that $\lambda_b = 0$ as well, one obtains:

$$\alpha + \beta = \frac{\mu_b + \beta}{1 + K} \qquad (3.10)$$

where K describes the push from the rear.

Implications and predictions of the CCW *concept.* The CCW concept predicts that a high ratio between basal and internal friction increases,

whereas a low ratio decreases the critical taper. Similarly, a high fluid pressure inside the wedge decreases its strength and increases thus the critical taper, while a high fluid pressure along the basal detachment decreases the basal strength and thus decreases the critical taper.

A taper stability field ($\alpha - \beta$ space) is defined by the basal and internal coefficients of friction (Dahlen, 1984), whereby cohesion and fluid pressure are neglected. Wedges in region I and III fail by thrusting or by a combination of thrusting and normal faulting because the frictional traction on their base is too great (Fig. 3.7). The resulting deformation acts to increase the taper of wedges in region I and to decrease it in region III. Wedges in regions II and IV are unstable as well, since the friction on their bases is too weak. They both fail by normal faulting, decreasing their taper in region II by gravity spreading and increasing it in region IV. Any wedge in the stability field is stable as long as the basal friction remains constant. An increase of the magnitude of basal friction causes regions I and III to grow and regions II and IV to

shrink in size. It follows that the stable regions decreases in size and ultimately disappears as the limit $\mu_b = \mu_0$ is approached (Dahlen, 1984).
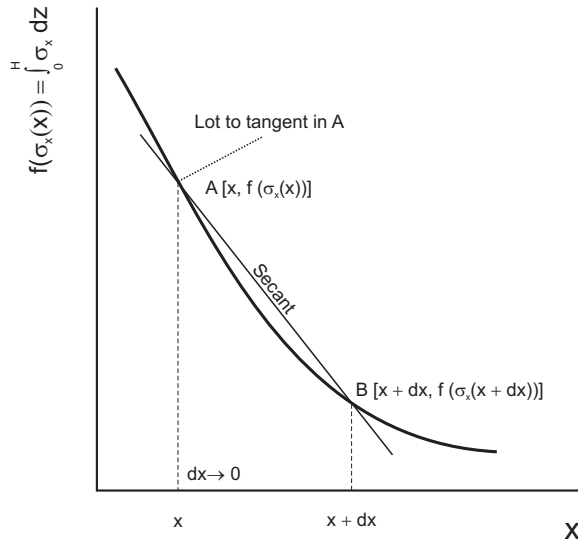

Figure 3.6: Relation between x position and a hypothetical solution of $f(\sigma_x(x)) = \int_0^H \sigma_x \, dz$, which is the work needed to push a plane perpendicular to x-axis at position x. This work is counteracted by forces acting on the plane at position $x+dx$. However, the latter is somewhat smaller than the former, since the push is coming from the thick end and the x-face is larger in area at x than at $x+dx$. The resultant force pushing the wedge towards the thin end, can be thus considered as the gradient of the secant (between A and B). If $dx \to 0$ is given, one obtains the gradient of the tangent at A and thus the push from the thick end at position x.

Surface processes tend to perturb the critical topographic form and may thus control the propagation and distribution of deformation within an orogenic wedge (Fig. 3.7). Outward propagation of deformation towards the foreland is more likely to occur in regions where erosion cannot maintain the surface gradient at or below a critical taper, or where enhanced sedimentation within intramontane basins adds to the thickness of the orogenic wedge (Schlunegger, 1999; Hovius, 2000). In contrast, erosion decreases the thickness of the wedge, which is equivalent to a decrease in the strength of crustal faults and thus drives continued internal deformation until the critical taper is restored (Davis et al., 1983; Dahlen and

Suppe, 1988; Willett, 1999). Correction of the perturbed topographic shape back to its critical state may also lead to changes in the pre-existing morphology, the pre-existing drainage pattern and the erosion rates which may finally trigger different modes of deformation.

The CCW concept has also been employed to predict the distribution and magnitude of fluid pressures, the velocity field and the distribution of metamorphic facies within accretionary wedges as well as their thermal structure (Dahlen and Barr, 1989; Barr and Dahlen, 1989; Barr et al., 1991). Furthermore, Hilley et al. (2004) and Hilley and Strecker (2004) used the CCW concept in conjunction with fluvial incision laws to show how a critically tapered orogenic wedge, which is in an erosional equilibrium, evolves through time. Probably the most important implication of the CCW concept is based on the fact that it does not depend on the across-strike position x, which means that critical wedges are scale invariant, i. e., $\alpha + \beta = constant$ (Davis et al., 1983; Dahlen and Suppe, 1988). The mechanics of orogenic wedges can thus be explained with the same concept used for snow or sand wedges. The above relation also indicates that critical wedges remain constant in shape but grow in size. A direct link between wedge shape and the orientation of the principle stresses is provided by:

$$\alpha + \beta = \Psi_b - \Psi_0 \qquad (3.11)$$

where the angle between the maximum principle stress σ_1 and the rigid base or the surface slope is denoted by Ψ_b for the former and by Ψ_0 for the latter (Davis et al., 1983).

A self-similar evolution of a crustal wedge implies also that the depth to the basal detachment increases with time. Such a scenario has been proposed for Taiwan by Davis et al. (1983). Based on the above result Dahlen and Suppe (1988) showed that the width and the height of critically tapered wedges grow proportional to convergence or time t by $t^{0.5}$ (Dahlen, 1990).
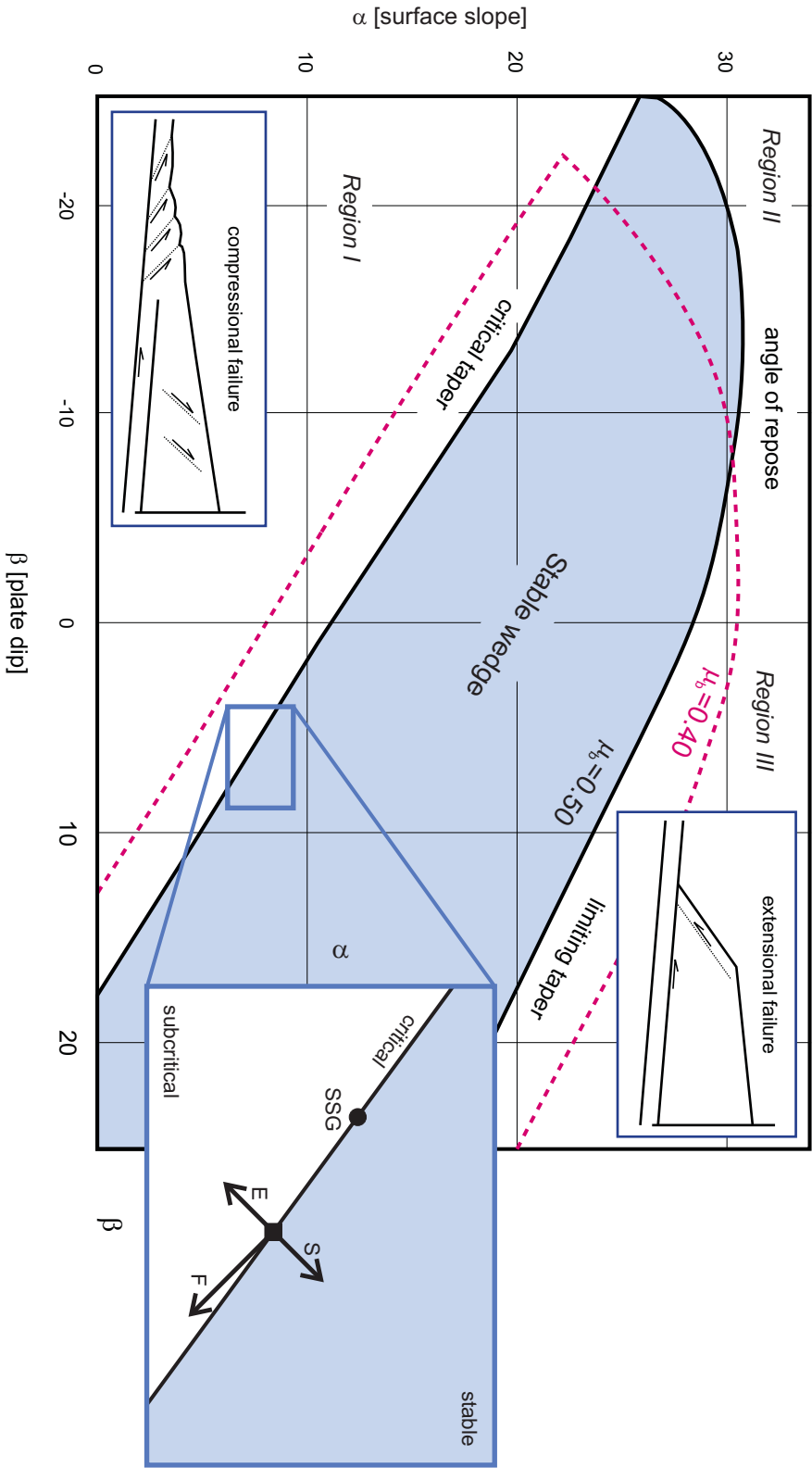
Figure 3.7: Taper stability field for two wedges with $\mu_b = 0.5$ and $\mu_b = 0.4$ and the four regions of non-stability. See text for explanation (page 21). Region IV not shown is located in the lower left corner. Modified after Dahlen (1984). Inset depicts influence of some key parameters: erosion of upper surface (E), Sedimentation or increased resistance to erosion (S) and flexural subsidence (F). Self-similar growth (SSG) of a certain wedge is shown as well. Modified after Horton (1999).

Although the predictive power and generality of the CCW concept is evident, it "only" provides quasi-static solutions for the geometry and stress states of wedges, but does not make any predictions about the deformation or the kinematics within deforming wedges (Willett and Pope, 2004). Thus, the often cited modes of internal thickening such as synchronous and out-of-sequence thrusting as well as basal accretion or back rotation may or may not be a consequence of the CCW concept (Boyer, 1995). As outlined above, the CCW concept assumes a linear Mohr-Coulomb failure criterion, which seems to be an oversimplification since rocks exhibit pre-failure strain-hardening and post-failure strain-softening (e. g., Mandl et al., 1977; Lohrmann et al., 2003), which promotes the re-activation of thrusts. It might follow, that the CCW concept should only be applied to the frontal part of a wedge (Lohrmann et al., 2003).

3.4 The minimum work concept of mountain building

The minimum work concept provides an alternative view on mountain building. Its conceptual simplicity in combination with its potential to predict the spatial and temporal distribution of deformation, an issue, which cannot be resolved with the CCW concept, has attracted many workers (Masek and Duncan, 1998). This concept assumes that the combined gravitational and frictional work associated with each slip increment along a set of faults is minimised. Thus, the fault which consumes the least work to accommodate slip is "chosen" (Fig. 3.8). Prolonged slip along a fault induces a negative feedback, since the gravitational load increases with every new slip increment. At a certain stage, the initiation of a thrust within the foreland would consume less gravitational and frictional work to accommodate further convergence. Thereby, the magnitude of work needed to initiate a fault depends on

the depth to its detachment, the internal and basal properties of the material and finally on the fluid-pressure (Davis et al., 1983; Hardy et al., 1998).
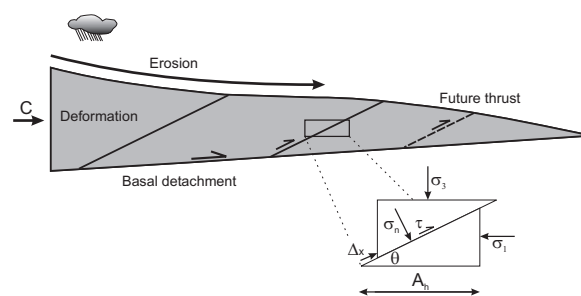

Figure 3.8: Schematic diagram of the minimum work concept and the parameters used to calculate the gravitational and frictional work. Modified after Hardy et al. (1998). C, external displacement rate; θ, local dip of the fault; Δx, fault parallel displacement; A_h, area of the fault plane projected onto the horizontal plane; σ_1, maximum; σ_3, minimum principal stress; τ, critical shear stress across the fault surface and σ_N, normal stress acting on this fault.

Although it is not appropriate to invoke a priori a minimisation principle to justify geological modelling, several studies have successfully demonstrated that the minimum work concept provides good approximations for specific aspects of mountain building; among them: the evolution of foreland duplexes (Mitra and Boyer, 1986), the lateral expansion of plateaus (Molnar and Lyon, 1988), the formation of triangle zones in fold and thrust belts (Jamison, 1993), the evolution of fold and thrust belts subject to erosion/sedimentation (Hardy et al., 1998), the initiation of thrusts within an accretionary wedge (Gutscher et al., 1998) and the interaction between erosion and plateau formation (Gerbault and Garcia-Castellanos, 2005).